13th World Conference on Earthquake Engineering
Vancouver, B.C., Canada
August 1-6, 2004
Paper No. 1958

SEISMIC COLLAPSE BEHAVIOUR OF DAMAGED DAMS

O. A. PEKAU[1] and Yuzhu CUI[2]

SUMMARY

In recent years much work has been reported on the formation and propagation of cracks in concrete gravity dams. In the case of the Koyna dam damaged during the 1967 earthquake, both analysis and field observations indicated that cracks penetrated though the full width of the dam. In this paper the subsequent seismic safety of such damaged dams is investigated. In particular, a comprehensive study on the dynamic behaviour of the fractured Koyna dam during earthquakes is performed using the distinct element method (DEM). The extensional functions of earthquake input and hydrodynamic simulation have been incorporated into the current program. The method of choosing the damping by the properties of each part of the system is discussed in detail. The whole failure processes of the two possible failure modes of the cracked dam, i.e. overturning or sliding of the separated top block during earthquakes under abnormal conditions, are also simulated. Some important phenomenon such as the bounce of the top block and the relationship of the sliding and overturning are examined in detail. It is concluded that horizontal and upstream-sloped cracks have a large margin of safety, whereas downstream-sloped cracks lead to early collapse under subsequent ground motion.

INTRODUCTION

The Koyna dam is a 103 m high gravity structure, which was visited by a strong earthquake of magnitude 6.5 on December 11, 1967. During this earthquake the dam suffered severe distress comprising horizontal cracks on both the upstream and downstream faces on a number of non-overflow monoliths. Leakage from some of these cracks was also found, which implied that the dam had been fully penetrated.

Linear analysis [1, 2] revealed that large tensile stresses in excess of the strength of concrete would develop in the dam during such strong earthquakes. Following these, much nonlinear analysis has been carried out to predict the occurrence and propagation of the cracks. The approaches used can be divided into two categories by means of how the cracks are modelled.

The first method, usually named the discrete crack approach, models the crack by separating the nodes belonging to crack flanks. Using the maximum tensile-strength criterion Skrikerud and Bachmann [3] simulated the crack propagation of Koyna dam under strong earthquakes by the discrete crack approach incorporated in a finite element method program, while Ayari and Saouma [4] studied this topic based on

[1] Professor, Concordia University, Montreal, Canada. Email: oapekau@civil.concordia.ca
[2] Post-doctoral Fellow, Concordia University, Montreal, Canada.

linear elastic fracture mechanics. Employing the boundary element model Pekau et al. [5, 6] investigated the progress of one discrete crack and multiple cracks in the dam, which was also based on linear fracture mechanics.

Another model is the so-called smeared crack approach, where the properties of the material in the zone of cracking are modified to represent the physical discontinuity introduced in a system by cracks. Pal [7] considered the effect of cracking on the response of Koyna dam by the finite element method with stress release once the tensile stress reached a critical value. Studies [8, 9] based on non-linear fracture mechanics models considering strain softening behavior in the fracture process zone have also been implemented, while other researchers [10, 11] have contributed by introducing damage mechanics into such analysis.

All of the studies have demonstrated the formation of cracks on both faces during the 1967 Koyna earthquake. And the most recent results also indicated that cracks near the change in downstream slope were expected to penetrate through the dam section. Although abundant results have been achieved, they mainly focused on the process of the crack occurrence and propagation. Since cracks are expected to have run through from upstream to downstream in some non-overflow sections of the dam splitting it into two totally separated blocks, the top block's stability in future severe earthquakes should be studied carefully. In 1974, Saini and Krishna [12] studied this problem assuming no sliding of the top block, which was regarded as a rigid body, neglecting the interaction between the top and bottom blocks and adopting a horizontal crack. Their results showed that under these assumptions the top block remained stable and overturning of the top profile would not occur under future ground motion of similar magnitude.

However, the top part is relatively large, and the interaction between the two blocks may have large influence on their behavior. Furthermore, from recent research [13, 14] the upper block also may slide along the top face of the lower one, whose length is limited. Then, the interaction behavior would change considering that the interface area of the blocks will decrease and the contact relations will change with the sliding of the upper block. The research of the crack propagation above demonstrated that the penetrated cracks may be shaped to exhibit upstream-slope or downstream-slope. Since there are many cracks along both the upstream and downstream faces, one cannot be sure that there are no cracks with downstream-slope, which can be expected to be most critical to the safety of the dam and should therefore be studied in detail also.

With the significant development of continuum and discontinuous media methods, such as the distinct element method (DEM) [15] or the discontinuous deformation analysis method (DDA) [16] in the past thirty years, it becomes not very difficult to study the stability of fractured dams in strong earthquakes while including the considerations mentioned above. An analysis on response of Pine Flat Dam during earthquakes with penetrated cracks was reported by El-Aidi and Hall [17] using the finite element method but limited in scope to small deformation of the continuum. To simulate the failure process of the fractured dam, discontinuous media methods have to be introduced.

In this paper, the distinct element method, which was proposed by Cundall in 1971 [15], is used to simulate the whole motion process of the Koyna dam with penetrated cracks during earthquakes. This method is capable of simulating the slip and separation behavior of contact joints and also the deformation of block elements. Since explicit time marching scheme is assumed for solving the dynamic equilibrium equations, it is suitable for nonlinear dynamic problems considering different kinds of boundary conditions. Because of these advantages, since its emergence DEM has been improved rapidly from rigid model to fully deformable, from two-dimensional to three-dimensional, and applied widely to engineering problems associated with stability analysis of high rock slopes, collapse simulation of structures, and underground works.

Although the distinct element method is well developed, there is still a problem in analyzing structures by this method due to the difficulty in choosing the damping of the system. In conventional analysis, a set of uniform damping coefficients for a system are usually used, which is reasonable when there are many blocks since the damping can be regarded as the mean value of all the blocks; however, this does not work well here. Considering that the top block above the penetrated crack and the lower one behave totally differently, different damping coefficients should be chosen respectively. Furthermore, the mechanism of the dashpots for the springs between blocks is very different from material damping and should be discussed separately. The simple idea of choosing the damping for the system turns out to be a key element of the study.

In this paper the main feature of the distinct element method is first described briefly, and the extensional functions of earthquake input and hydrodynamic simulation are incorporated into the current program [18]. Then following the discussion of the damping systems, responses of the fractured Koyna dam during the earthquake of 1967 are studied in detail for three different shaped cracks. Examined in particular are the failure processes comprising the two possible failure modes of the cracked dam, i.e. overturning and sliding of the top separated block during severe ground motions.

DISTINCT ELEMENT METHOD (DEM)

The system in DEM is divided into blocks by joints and, furthermore, the blocks are assumed to be fully deformable and discretized into triangular constant-strain elements by the automatic mesh generator incorporated in the DEM program [18] for stress-strain analysis. Normal and shear springs and dashpots are set between contact blocks for simulating the behavior of joints. Technologies such as rounded corners and 'domain'-based algorithm presented by Cundall [19] are used for contact detection.

Explicit time marching scheme is assumed to solve the dynamic equilibrium equations. In each time step, the motion of each node of all the blocks is prescribed individually by the following equation for the case of mass proportional damping and gravity:

$$m\ddot{u} + \alpha m\dot{u} = F + mg \tag{1}$$

where m is the mass lumped at a node whose value is the sum of the masses of all the elements around the node divided by 3. That means the inertial mass of each triangular element is equally distributed to the three vertices. α is the mass proportional damping coefficient and g is the gravity acceleration. $\ddot{u}$ and $\dot{u}$ denote the acceleration and velocity of the node, respectively. F represents the summation of forces applied at the node including contact forces, elastic forces, damping forces and possibly boundary forces. By employing the central difference method for acceleration $\ddot{u}$, this equation can be solved explicitly to obtain new velocities and displacements at the end of each time step from the beginning values. Here, boundary motions can be imposed easily. After the motions of each node are determined, the new elastic forces and contact forces can then be obtained by employing the corresponding constitutive relationships, leading to the total force for the next time step.

Various contact constitutive behaviours of joints can be incorporated easily in the spring-dashpot model. The elastic one following Coulomb's friction law with zero tension in the normal direction expressed below is used [18]:

$$
\begin{aligned}
&F_c^n = k_n u_n \qquad if\ u_n \le 0 \\
&F_c^n = 0 \qquad if\ u_n > 0 \\
&F_c^s = k_s u_s \qquad if\ \left|F_c^s\right| \le f\left|F_c^n\right| + cL \\
&F_c^s = sign(u_s)(f\left|F_c^n\right| + cL) \qquad if\ \left|F_c^s\right| > f\left|F_c^n\right| + cL
\end{aligned}
\tag{2}
$$

where k_n and k_s are the normal and shear spring stiffnesses representing the elastic joint properties. F_c^n and F_c^s are the normal and tangential components of the contact force, respectively and u_n and u_s are the corresponding components of the relative contact displacement. f, c are the friction and cohesion coefficients of the joint material and L denotes the length of the contact boundary.

The forces of the normal and shear dashpots F_{dc}^n and F_{dc}^s related to the relative velocity of the blocks at contact can be described as

$$
F_{dc}^n = -\beta k_n \dot{u}_n = -\beta \frac{\Delta F_c^n}{\Delta t}, \qquad F_{dc}^s = -\beta k_s \dot{u}_s = -\beta \frac{\Delta F_c^s}{\Delta t} \tag{3}
$$

where β is the stiffness proportional damping coefficient; ΔF_c^n and ΔF_c^s are the incremental normal and shear forces of a spring, respectively; and Δt is the time step.

For each triangular constant-strain element of the deformable blocks, its strain change is easily determined since the velocities of its three vertices are known. Then, by employing the stress-strain relationship, the incremental stress tensor $\Delta\sigma_{ij}$ and the new stress tensor σ_{ij} in each element is obtained. Here, various material constitutive relationships can be applied easily also, whereas an elastic linear one is used herein. The elastic force F_e at a grid point due to elastic deformation of the block can be obtained by integrating the stress along the mass boundary Γ of the corresponding grid point, where Γ is determined by the rule that inertial mass of each triangular element is equally distributed to its three vertices.

If stiffness proportional damping due to the elastic strain change of the block needs to be considered, it can be found by integrating the rate of the incremental stress tensor along the same route Γ:

$$
F_{de} = -\int_{\Gamma} \beta' \frac{\Delta\sigma_{ij}}{\Delta t} n_j ds \qquad i, j = 1,2 \tag{4}
$$

where n_j is the unit normal vector of the integration boundary and β' is the corresponding stiffness proportional damping coefficient different from β which is the coefficient of the contact dashpots between blocks. Therefore, their values may be set the same or not depending on the problem under consideration.

In the following simulation of Koyna dam's failure processes during strong earthquakes, earthquake input and hydrodynamic influence have to be considered. For seismic loads, the intuitive method by a large base block serving as a shaking table [20] or prescribing directly the motion of boundary nodes [18] can be employed. The former can be used only for uniform earthquake input, while the latter is also suitable for

non-uniform motion. However, one simple way, used in the following simulation, is to add a virtual inertial force to each corresponding node in the system while regarding the ground as fixed. The value of the force is the acceleration of the ground multiplied by the lumped mass of each node. It is difficult to analyze the dynamic behavior of the dam-reservoir system completely. Here, the influence of the reservoir when the dam is subject to earthquake excitation is represented by an equivalent virtual mass in the horizontal direction [21]. Thus, equation (1) becomes the following:

$$\begin{aligned} (m+m')\ddot{u}_x + \alpha(m+m')\dot{u}_x &= F_x + (m+m')g'_x \\ m\ddot{u}_y + \alpha m\dot{u}_y &= F_y + mg + mg'_y \end{aligned} \tag{5}$$

where subscripts x and y denote horizontal and vertical directions, respectively; g' represents the ground acceleration and m' is the virtual mass whose value varies for the nodes on the upstream face of the dam under water while remaining zero for the others.

NUMERICAL MODELS OF FRACTURED KOYNA DAM

DEM discretization, material parameters and loads

The cross-section of the highest non-overflow monolith of the dam shown in Figure 1(a) is 103 m high, 14.8 m wide at the top and 72 m at the bottom, with a sharp slope change on the downstream face at the level of 66.5 m.

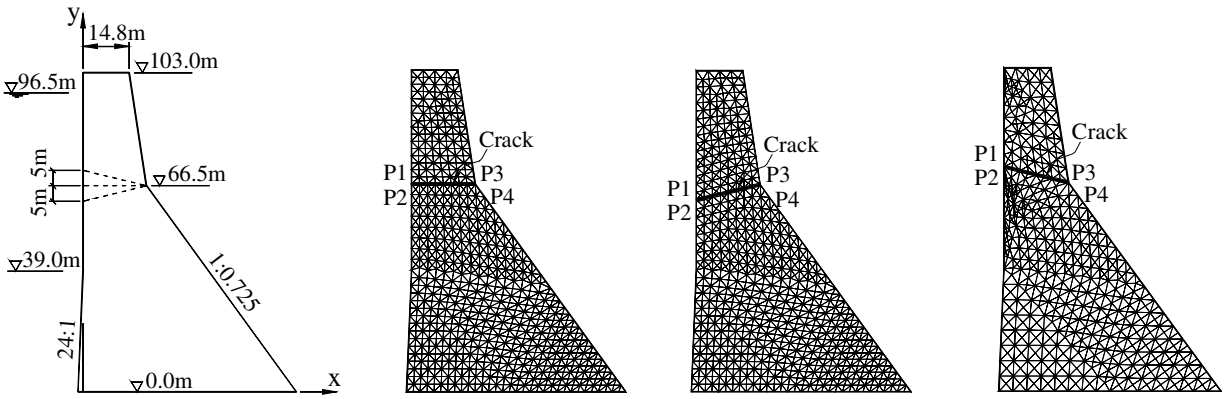

(a) Cross-section of dam (b) Horizontal crack: Case I (c) Upstream-sloped crack: Case II (d) Downstream-sloped crack: Case III

Fig 1. Details of fractured dam and DEM discretization

To analyze the stability of the top profile and its possible collapse modes three crack shapes, which will be analyzed in the following, are assumed as shown in Figure 1(a): horizontal crack, which was also assumed by Saini and Krishna [12] when analyzing the overturning of the top profile; upstream-sloped crack, which is 5 m high and simplified based on the results in reference [5]; and downstream-sloped crack, which mirrors the upstream-sloped crack over the horizontal. Their corresponding DEM discretizations are depicted in Figures 1(b), 1(c) and 1(d) and titled as Case I for the profile with horizontal crack, Case II for the upstream-sloped crack and Case III for the downstream-sloped crack. In all cases, the profile of the dam is divided into two deformable blocks by the corresponding assumed crack. The triangular constant-strain elements for stress-strain analysis in each block are automatically discretized by the program. Points P1 and P2 are at the left end of the crack and belong to the top and the bottom block, respectively, and similarly points P3 and P4 are at the right end of the crack.

Parameters of the Koyna dam concrete are the following: elastic modulus $E = 3.1\times10^{10}$ Pa; mass density ρ = 2640 kg/m^3; and Poisson ratio ν = 0.2. The cohesion coefficient of the crack is set at zero, considering that once the block slides along the crack its value should become very small. The friction coefficient is set at 1.0, and its influence with different values will be discussed also. There are no test values for the stiffness of the springs k_n and k_s, which represent the elastic property of the crack. They are assumed equally as 2.0×10^9 N/m, approximately one fifteenth of the value of the elastic modulus of the concrete blocks.

The nodes in the bottom face of the lower block at level 0.0 m are fixed, and maximum reservoir water level of 96.5 m is considered. Applied loads include self-weight of the dam, hydrostatic, hydrodynamic, uplift and earthquake forces. Hydrodynamic loads are added by the aforementioned method of virtual mass and the value of the virtual mass m_i' at node *i* on the upstream surface of the dam is [21]

$$m_i' = \frac{7}{8}\sqrt{hy_i}\,\rho_w(b_{i1}+b_{i2})/2 \tag{6}$$

where y_i and *h* are the distance from node *i* to the water surface and the depth of water, respectively; ρ_w is the mass density of water; and b_{i1} and b_{i2} are the length of the edges of the triangular constant-strain elements beside node *i* on the upstream surface of the dam. Uplift pressure is added along the crack to both the bottom of the upper block and the top of the lower part and assumed conservatively as full water pressure without discount [12], which shows a rectangular shape of water pressure in Case I, and trapezoidal in both Cases II and III. The recorded Koyna ground acceleration on December 11, 1967 is used, whose peak value is 0.49 g in the stream direction and 0.34 g in the vertical direction. Time step $\Delta t = 1.7\times10^{-4}$ s is assumed in the computations of Cases I and II, while 4.4×10^{-5} s is employed for Case III because the elements for this case are not as uniform as for the former two.

Damping system

Damping is very important to the behavior of the fractured dam during earthquakes, especially to the top block. Since the profile has been separated completely into two parts by the crack and their behaviors are totally different, it is reasonable to choose the damping for the blocks separately. The dashpots for the springs connecting the separate blocks will dissipate energy when there is impact between them. Thus damping of the system can be divided into three zones and selected according to the behavior of corresponding parts as depicted schematically in Figure 2.

For the lower block, it can be considered as a common structure fixed along its bottom face while the top block is regarded as its boundary condition. Its mass proportional damping α_1 is set to 2.1 for equivalent viscous damping ratio ξ = 0.05 at the first modal frequency of 6.63 Hz, while the stiffness proportional damping β_1 is assumed as zero. The top block behaves nearly as a rigid body during earthquakes, and its mass and stiffness proportional damping α_2 and β_2 should be very small. Hence they are set conservatively to zero.

However it is difficult to determine the value of the dashpots β, since it represents the property of the crack and the mechanism of the energy dissipation during impact, which is very complex. Here, it is chosen by numerical test. Considering that the damping coefficients α_2 and β_2 have been set to zero,

there are only two ways remaining to dissipate the energy of the top block, namely through friction and impact with the lower part. When both the coefficients of friction *f* of the crack and of the dashpots β are very low, the energy then will not be dissipated properly. This can be seen from the displacement histories of point P1 in Case I with different values of β as shown in Figure 3, where the friction coefficient *f* of the crack is set as 0.5 near the static critical value of 0.416. For small value of β (0.0012) the movement of the top block continues to increase after the earthquake (ended at 11 s) under the horizontal water pressure and uplift, which is not reasonable. When β is 2, 3 and 4 times this value, i.e. 0.0024, 0.0036 and 0.0048, respectively, the displacement of point P1 becomes steadily stable after the earthquake in all cases. The permanent sliding of the top block becomes smaller when the value of β becomes larger. However, because of the complication of impact due to interactions between the two blocks and their deformations themselves, the same trend is not seen for the vertical component of the displacements. Although the value of β has large influence on values of the results, in the following simulation only the value of 0.0036 is chosen since nearly the same trends appear with different proper values of β by separate calculations.

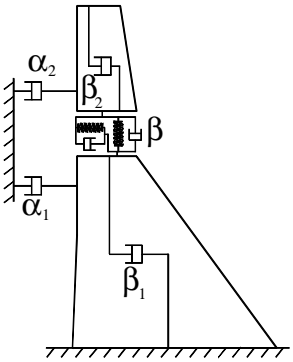

Fig 2. Schematic of damping system

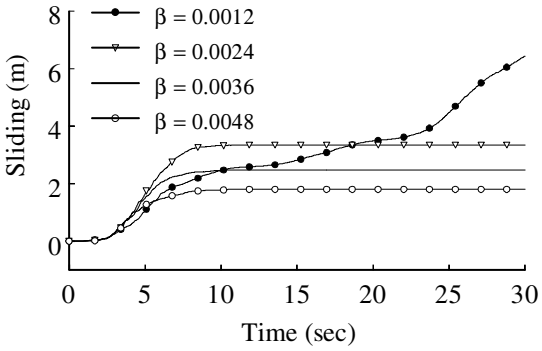

Fig 3. Sliding of point P1 with different contact damping in Case I (*f* = 0.5)

FAILURE ANALYSIS AND COLLAPSE PROCESS SIMULATIONS

Response of dam during 1967 Koyna earthquake

The motion histories of the top block during the Koyna earthquake for the three cases with different kinds of penetrated crack are shown in Figure 4. As seen, the top block behaves totally differently in each case. In Case III, the top block slides along the downstream-sloped crack steadily as shown in Figure 4(a), and comes into collapse with its displacement in rotation in Figure 4(b) increasing rapidly after 6.5 s, whereas the top block remains stable in Case I with horizontal crack and Case II with upstream-sloped crack. After the earthquake, a comparatively large permanent sliding displacement along the crack of the top block is found in Case I while the corresponding value is very small and no more than 0.1 m in Case II, because the upstream-sloped crack increases the resistance against downstream sliding of the top block. It is interesting to note that the rotation frequency is very similar in these three cases as shown in Figure 4(b), although the intensity is quite different. The rotation oscillation is very severe in Case III, whose peak value reaches 0.016 radians at about 5 s before the collapse of the top block. The maximum rotation of the top block happens at almost the same time in Case I with the value of 0.0056 radians, while in Case II it only reaches 0.0027 radians at about 4.2 s.

The collapse process of the top profile in Case III is shown in Figure 5. The top block has moved more than 3.5 m downstream at 5 s, and before this point its main motion is sliding along the crack. At 8 s it has

already rotated by a large angle around the support point P4 of the lower block corner and come into collapse. At 10 s the top block's centroid has passed the support point, and the block begins to fall as a free falling object. Within 5 s it reaches the ground. From this failure process, and together with the motion histories of the top block in Case III from Figure 4, one can see that rotation is accompanying the sliding. After large sliding, the top block comes into collapse and rolls down the downstream face of the dam. Since they have large influence on each other, it is important to analyze these two kinds of motion, rotation and sliding, at the same time.

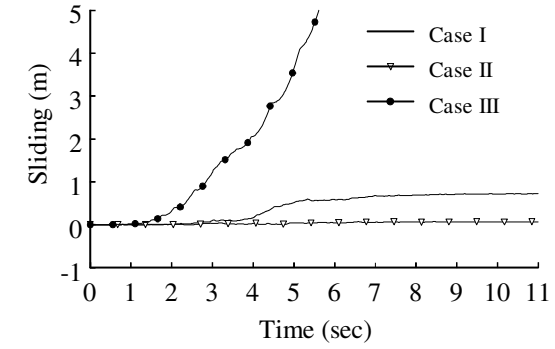

(a) Sliding along the crack of point P1

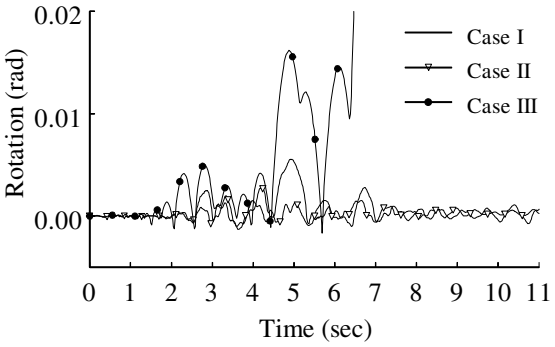

(b) Rotation

Fig 4. Movement histories of top block for different cases of fracture

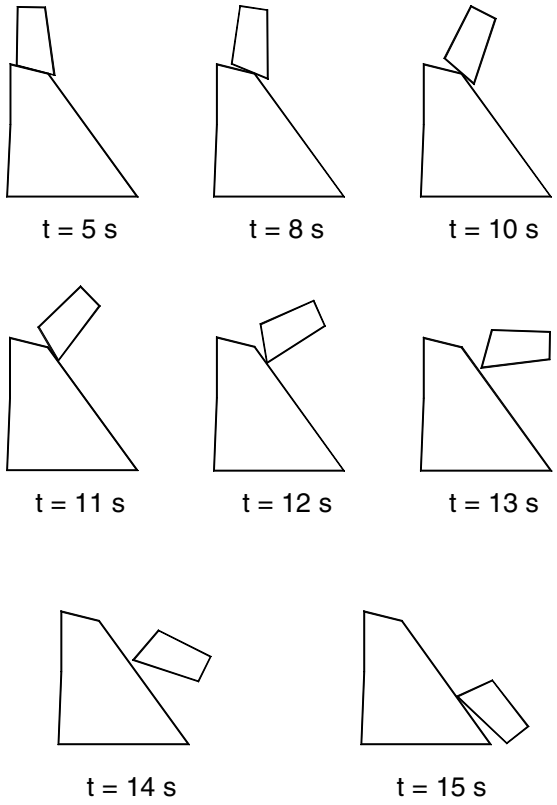

Fig 5. Process of dam failure under earthquake for Case III

Figure 6 presents the opening and closure histories of the crack for stable Case I. The opening at the upstream end is dominant compared with that at the downstream end. This is mainly because the force of the water pressure on the upstream face of the dam makes the top block easier to rotate toward downstream rather than upstream. Consistent with the rotation histories of Figure 4(b), the peak opening of the crack at the upstream end happens at 4.9 s, reaching 0.11 m, while the crack is closed at the other end.

Although usually joints at the upstream and downstream ends open alternately, or both close, there are still moments in time that they open together at the same time for an instant, which is very clear in Case I. For example at the time of 3.7 s, the crack opens 0.021 m at the upstream end and 0.033 m at the downstream end, and at 4.4 s 0.030 m at the upstream end and 0.024 m at the downstream as seen in Figure 6. This means that the top block bounces away from the bottom section completely at these times. Thus, even though the friction coefficient of the crack is high, it cannot prevent the top block from sliding during the free flight of the bounce since there are no contact forces, and hence no resistance against sliding

downstream under water pressure at such moments. The separation does not continue for long, only about 0.2 s or so, and the crack then closes quickly under the weight of the dam. Clearly this phenomenon poses the potential of causing high hydrodynamic pressure inside the crack.

The profile of the crack at 4.9 s when the rotation of the top block reaches the maximum of 0.0056 radians is shown in Figure 7, and Figure 8 shows its bounce at 3.7 s. The diagrams have been amplified 20 times in the y direction to show the opening of the crack clearly.

From the above, one can see that the fractured Koyna dam can be stable in earthquakes the same as occurred in 1967 with the crack shaped horizontal as in Case I or upstream-sloped as in Case II while unstable with downstream-sloped crack as in Case III. However, even in the stable cases the top block will slide along the crack a certain distance, especially in Case I, and be accompanied by small rotations. It may even separate from the lower part for an instant during the earthquake.

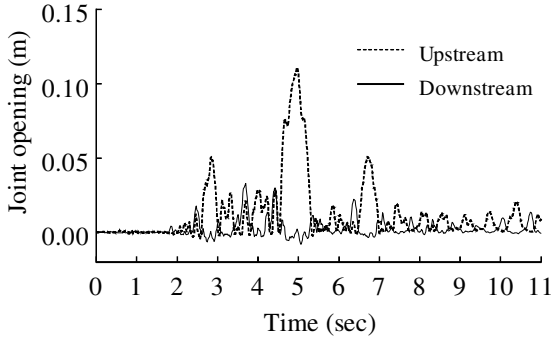

Fig 6. Opening and closure of joints during earthquake

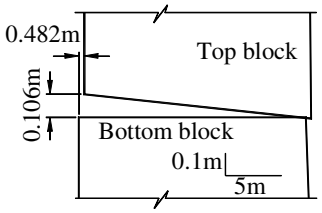

Fig 7. Crack profile at 4.9 s

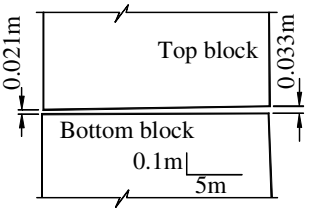

Fig 8. Crack profile at 3.7 s

Failure analysis of the top profile under abnormal conditions

Although the fractured dam with horizontal or upstream-sloped crack can be stable under the 1967 Koyna earthquake as seen above, it is important to examine its collapse process under different abnormal conditions. Such a study will be helpful not only to estimate the actual margin of the dam's safety but also to understand the failure mechanism itself. In the following, the earthquake input and the coefficient of friction of the crack are varied for such analysis.

Increasing the intensity of earthquake

Keeping the coefficient of friction of the crack at 1.0, the intensity of the earthquake is increased until the collapse of the top profile in each of Cases I and II is obtained. The displacement histories of the top block during earthquakes with different intensity, which was obtained by multiplying the 1967 Koyna earthquake by factors of 1, 2, 3 and 4, are shown in Figure 9 for Case I. The associated collapse process, when the earthquake is 4 times the severity of the original, is depicted in Figure 10. The corresponding results of Case II are presented in Figures 11 and 12 where the dam comes into failure only when the earthquake intensity increases to 7 times original.

As seen from Figures 9 and 11, when earthquake intensity increases, the response of the top block becomes more severe, and the maximum rotation and the permanent sliding displacement usually increase also. However, due to the strong nonlinear property of this problem, there are some exceptions; for example, in Case I, the permanent sliding displacement under the earthquake with intensity 2 times original is slightly larger than that of 3 times.

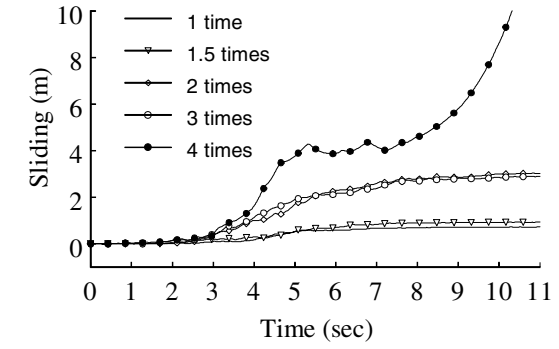

(a) Sliding along the crack of point P1

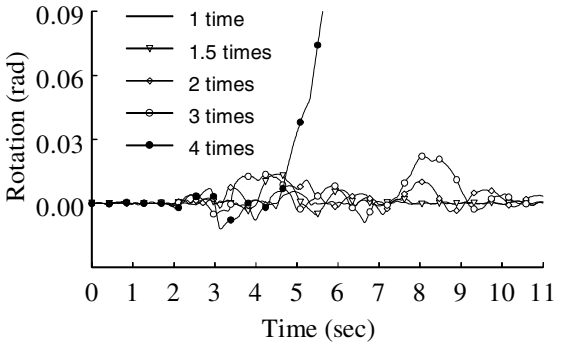

(b) Rotation

Fig 9. Movement histories of the top block during earthquake with different intensity for Case I

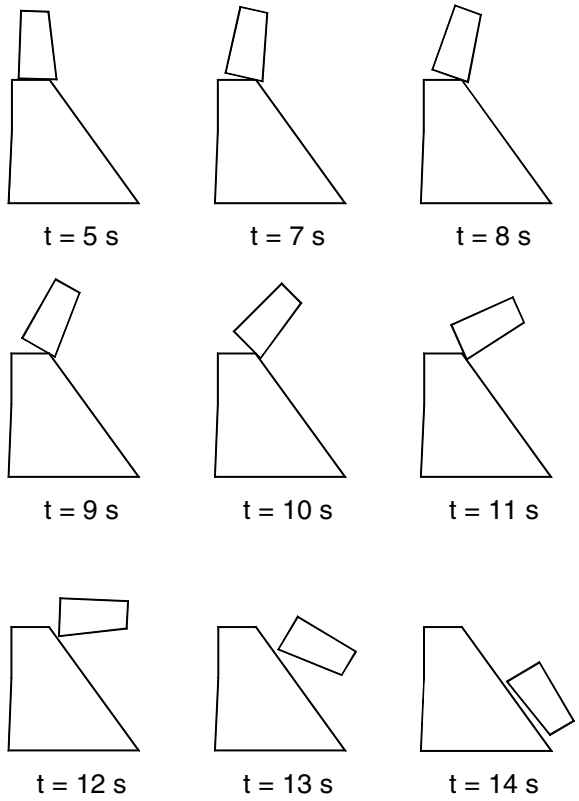

Fig 10. Process of dam failure under earthquake for Case I (intensity of earthquake 4 times original)

During the earthquake, the top block mainly slides downstream along the crack in Case I, which is clear from Figure 9(a) where the displacement of the top block along the crack at point P1 increases steadily before collapse. In Case II, because the crack dips up-stream which makes it easier to slide down the slope, the top block exhibits apparently reverse sliding during earthquakes. As seen from Figure 11(a), the displacements of the top block along the crack at point P1 have large relative increases and decreases, and for the curves under earthquakes with intensity 6 and 7 times original the value even decreases to minus, which means that the top block slides upstream from its original position. This also can be seen clearly from the failure process at 4 s in Figure 12, when the top profile deviates upstream. Also in Figure 12, comparing the position of point P4 to point P3 in pictures of 6 s and 7 s one can see that the top block slides a certain distance upstream while rotating around the point P4, which is consistent with the big decrease between 6 s and 7 s of the curve of the failure case in Figure 11(a). Thus, even if the top profile collapses downstream, this may be accompanied by significant upstream sliding.

In Case I, the collapse of the top profile can be considered to begin at 4.8 s from where its rotation increases steadily without stop as seen in Figure 9(b), while the point for Case II is at about 6 s as seen in Figure 11(b). Before these points, the top block has slid a large distance (more than 3 m) downstream along the crack in both cases as seen in Figures 9(a) and 11(a). The sliding makes the overturning of the top block easier since the interface of the upper and lower part of the dam becomes much smaller than original, and the arm of the gravity of the top block against rotation to the support point P4 becomes 3 m shorter. So, even for the overturning failure mode, the sliding of the top block plays an important role.

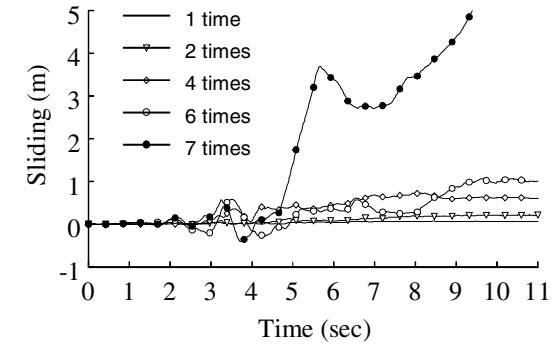

(a) Sliding along the crack of point P1

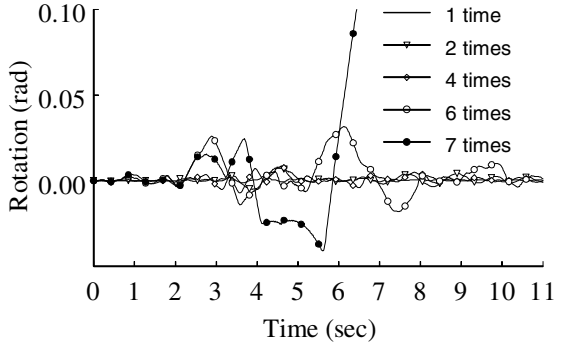

(b) Rotation

Fig 11. Movement histories of the top block during earthquake with different intensity for Case II

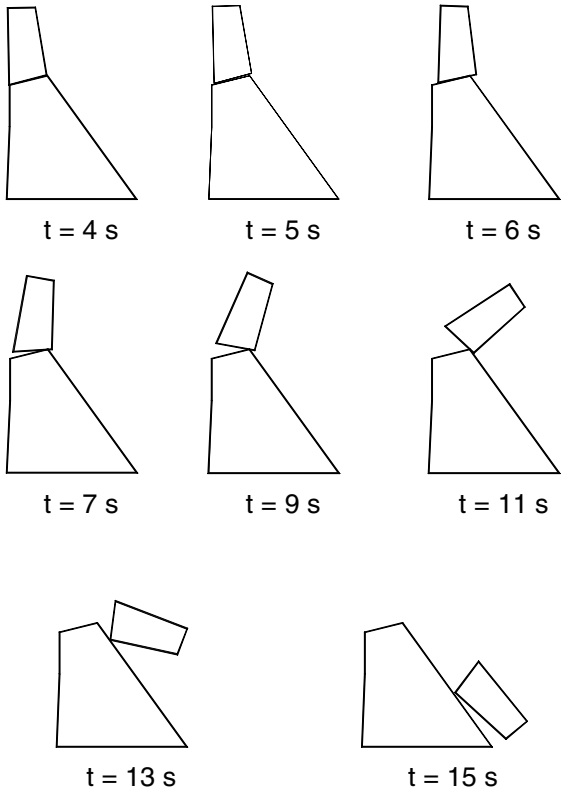

Fig 12. Process of dam failure under earthquake for Case II (intensity of earthquake 7 times original)

As seen from the profile at 5 s in Figure 12, the bounce of the top part of the dam from the lower one is clearly visible even without amplification in the y direction. Here also, it is evident that the hydrodynamic pressure in the crack, while not included here, may become an important factor.

Although the crack shape in each case is different and the earthquake in Case I is 4 times the original while 7 times in Case II, their failure processes are very similar as seen in Figures 10 and 12, and the collapse itself is very rapid being limited to a few seconds. As soon as the top block comes into collapse, it rotates quickly around the support point P4, and before the end of the earthquake its centroid has already passed by the support point, then falls to the ground in a few seconds as a free falling object.

Decreasing the friction coefficient f of the crack

While keeping the earthquake intensity as original, the friction coefficient of the crack is decreased until collapse of the top profile occurs in each of Cases I and II. For both cases, not until the friction is very low, almost at the static critical value, does the dam collapse under the earthquake. For Case I, the top profile comes into failure when the coefficient of friction of the crack decreases to 0.42, while the static critical value is 0.416 and, in Case II, to 0.13 for the dynamic case compared to 0.128 for the static.

The permanent sliding displacement and the maximum rotation of the top block under earthquake with different friction coefficient of the crack are given in Tables 1 and 2 for Case I and Case II, respectively. From these results, the main trend of the permanent sliding in both cases is nearly the same, namely that the displacement of the cracked block increases as *f* becomes low, although there are exceptions at some

values. However, the relationship between maximum rotation and friction coefficient is quite different between Cases I and II. In Case I, the maximum rotation seems random, whereas in Case II its value decreases with the friction value, although there is exception when f equals 1.2 since the problem is strongly nonlinear. Generally the permanent displacements under earthquake in Case II are much smaller than those in Case I, confirming that the profile with upstream-sloped crack is safer under the 1967 Koyna earthquake in such conditions than that with horizontal crack.

Table 1. Permanent sliding displacement and maximum rotation of the top block in Case I with different friction coefficient *f* of the crack

f	1.2	1.1	1.0	0.9	0.8
Displacement (m)	0.683	0.590	0.735	1.299	1.105
Rotation (radian)	0.00316	0.00295	0.00556	0.00481	0.00333

f	0.7	0.6	0.5	0.42
Displacement (m)	1.493	1.570	2.475	Unstable
Rotation (radian)	0.00600	0.00232	0.00644	

Table 2. Permanent sliding displacement and maximum rotation of the top block in Case II with different friction coefficient *f* of the crack

f	1.2	1.0	0.8	0.6
Displacement (m)	0.070	0.066	0.181	0.152
Rotation (radian)	0.00340	0.00270	0.00304	0.00187

f	0.4	0.3	0.2	0.13
Displacement (m)	0.367	0.511	0.848	Unstable
Rotation (radian)	0.00109	0.00090	0.00068	

The movement histories of the top block when it comes into failure with f decreasing to 0.42 for Case I and to the low magnitude of 0.13 for Case II are shown in Figures 13, and the corresponding collapse processes are presented in Figures 14 and 15.

From the above results, one can see that the failure process is very similar for both cases, and can be divided into two stages: the sliding stage and the collapse stage. The sliding stage ends when the top block has moved a long distance along the crack and caused the top block to become unstable even under static loads. Then the failure process comes into the second stage, namely rotation around the point P4 and falling down freely.

As seen in Figure 13(a), 12 s can be regarded as the end of the first stage of failure for Case I. Before this point, the displacement of the top block along the crack increases steadily, while the value normal to the crack remains around zero, and its rotation is also limited. The earthquake ends at 11 s; however because the friction of the crack is so low, almost at the static critical value, the top block continues to slide under the hydrostatic force on the upstream face. At the end of the first stage of 12 s, the sliding distance has already reached about 8 m when the top block comes into the collapse stage with rotation increasing rapidly. The failure process depicted in Figure 14 is consistent with the above behaviour. And when the centroid of the top block has passed the support point P4 at 16 s, it begins to roll down quickly.

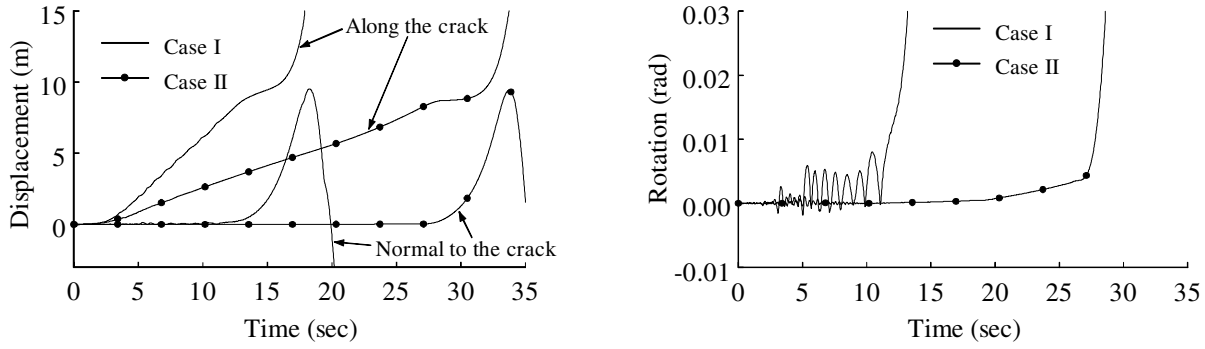

(a) Displacement of point P1 (b) Rotation

Fig 13. Movement histories of the top block (f = 0.42 for Case I and f = 0.13 for Case II)

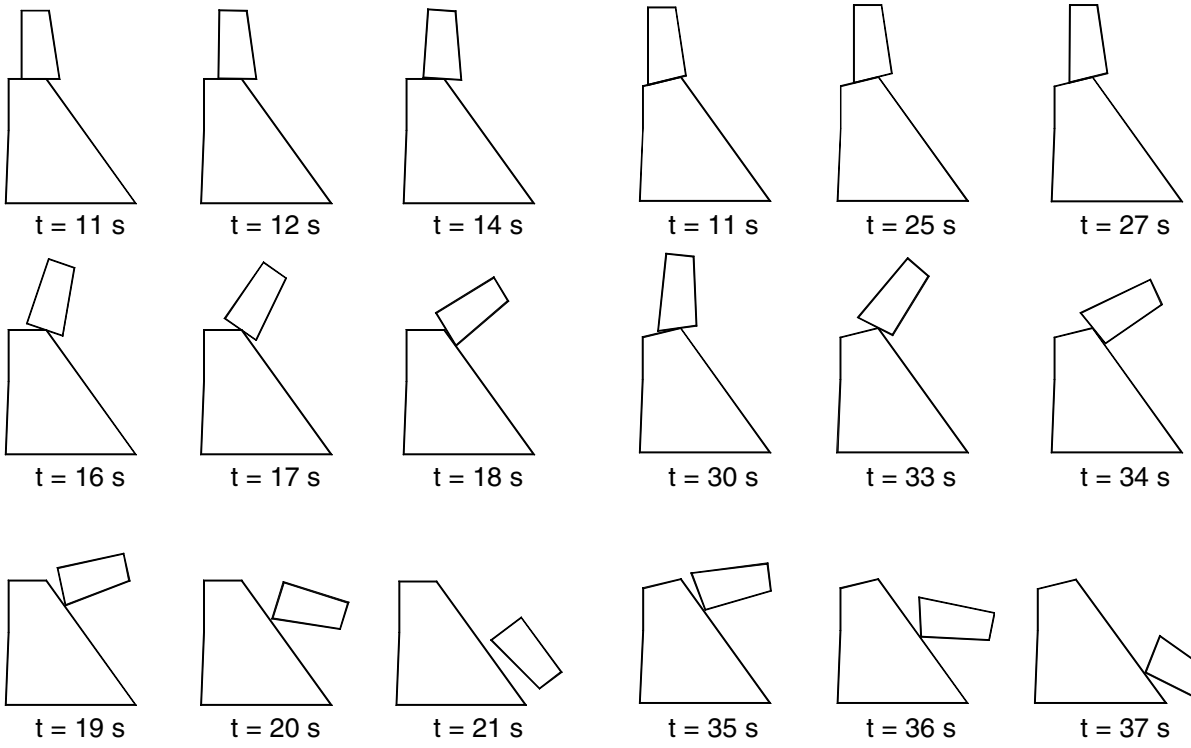

Fig 14. Process of dam failure with f = 0.42 for Case I

Fig 15. Process of dam failure with f = 0.13 for Case II

The whole failure process in Case II with f equal 0.13 is very similar to that of Case I, although the transition point is at about 27 s as seen in Figure 13. The rotation of the top block during the sliding stage is very small. And at the end of the earthquake at 11 s the sliding displacement is only about 3 m. However it reaches more than 8 m at 27 s, at which time the top block comes into the collapse stage with the resulting failure process depicted in Figure 15. Before 27 s, the top block shows almost no rotation, and its main motion is sliding along the crack. After 27 s, it begins to rotate around the support point P4 before falling down.

Summarizing the above failure processes, the two modes of failure, i.e. overturning and sliding are really possible only under abnormal conditions. Although from the results the dam has a very large safety margin

with horizontal crack or upstream-sloped crack, the sliding of the top block and the bounce phenomenon are distinct features of the behaviour.

CONCLUSIONS

1. Damping is a very important parameter for the DEM simulation, and has been assigned different values for different parts of the fractured dam.

2. Results show that the safety of the dam is ensured if the crack shape is horizontal or upstream-sloped, and it is very dangerous if the crack slopes downstream. For the latter the top block slides and then rolls down the downstream face even with high crack friction coefficient of 1.0. However, even with horizontal crack, the top block will bounce away from the lower part for a moment, which may introduce high hydrodynamic pressure in the water inside the crack. Thus, the property and shape of the crack needs be checked carefully in a fractured dam in order to assess a fractured dam's safety.

3. The top block will overturn, if the earthquake is abnormally strong such as 4 times the recorded Koyna earthquake of 1967 for profile with horizontal crack, or 7 times for upstream-sloped crack. For this kind of failure mode consisting of the top block overturning, the sliding of the top block is still an important factor, since the sliding denotes the first stage in the failure process preceding the overturning of the top block.

4. If the friction coefficient of the crack is abnormally low, large sliding displacement of the top block during earthquakes will also cause collapse of the dam. However, the dynamic critical value of the coefficient of friction is almost the same as the static one.

5. As concluded from 3 and 4, there is large margin of the safety for the dam with horizontal or upstream-sloped cracks.

ACKNOWLEDGEMENTS

The authors gratefully acknowledge the financial support of this work which was provided by the Natural Sciences and Engineering Research Council of Canada under Grant No. A8258.

REFERENCES

1. Chopra AK, Chakrabarti P. "The earthquake experience at Koyna dam and stresses in concrete gravity dams." Earthquake Engineering and Structural Dynamics 1972; 1: 151-164.
2. Saini SS, Krishna J, Chandrasekaran AR. "Behavior of Koyna Dam—Dec. 11, 1967 Earthquake." Journal of the Structural Division, ASCE 1972; 98(ST7): 1395-1412.
3. Skrikerud PE, Bachmann H. "Discrete crack modelling for dynamically loaded, unreinforced concrete structures." Earthquake Engineering and Structural Dynamics 1986; 14: 297-315.
4. Ayari ML, Saouma VE. "A Fracture mechanics based seismic analysis of concrete gravity dams using discrete cracks." Engineering Fracture Mechanics 1990; 35(1/2/3): 587-598.
5. Pekau OA, Feng LM, Zhang CH. "Seismic fracture of Koyna dam: case study." Earthquake Engineering and Structural Dynamics 1995; 24: 15-33.
6. Batta V, Pekau OA. "Application of boundary element analysis for multiple seismic cracking in concrete gravity dams." Earthquake Engineering and Structural Dynamics 1996; 25: 15-30.
7. Pal N. "Seismic Cracking of Concrete Gravity Dams." Journal of the Structural Division, ASCE 1976; 102(ST9): 1827-1844.

8. Bhattacharjee SS, Leger P. “Seismic Cracking and energy dissipation in concrete gravity dams.” Earthquake Engineering and Structural Dynamics 1993; 22: 991-1007.
9. Wang GL, Pekau OA, Zhang CH, Wang SM. “Seismic Fracture analysis of concrete gravity dams based on nonlinear fracture mechanics.” Engineering Fracture Mechanics 2000; 65: 67-87.
10. Ghrib F, Tinawi R. “An application of damage mechanics for seismic analysis of concrete gravity dams.” Earthquake Engineering and Structural Dynamics 1995; 24: 157-173.
11. Lee J, Fenves GL. “A Plastic-damage concrete model for earthquake analysis of dams.” Earthquake Engineering and Structural Dynamics 1998; 27: 937-956.
12. Saini SS, Krishna J. “Overturning of top profile of the Koyna dam during severe ground motion.” Earthquake Engineering and Structural Dynamics 1974; 2: 207-217.
13. Chopra AK, Zhang LP. “Earthquake-induced base sliding of concrete gravity dams.” Journal of Structural Engineering, ASCE 1991; 117(12): 3698-3719.
14. Chavez JW, Fenves GL. “Earthquake response of concrete gravity dams including base sliding.” Journal of Structural Engineering, ASCE 1995; 121(5): 865-875.
15. Cundall PA. “A Computer model for simulating progressive large scale movements in blocky rock systems.” Proceedings of the Symposium of the International Society for Rock Mechanics, Nancy, France. Vol. 1, Paper no. II-8. 1971.
16. Shi GH, Goodman RE. “Two dimensional discontinuous deformation analysis.” International Journal for Numerical and Analytical Methods in Geomechanics 1985; 9(6): 541-556.
17. El-Aidi B, Hall JF. “Non-linear earthquake response of concrete gravity dams Part 2: behaviour.” Earthquake Engineering and Structural Dynamics 1989; 18: 853-865.
18. Zhang CH, Pekau OA, Jin F, Wang GL. “Application of distinct element method in dynamic analysis of high rock slopes and blocky structures.” Soil Dynamics and Earthquake Engineering 1997; 16: 385-394.
19. Cundall PA. “UDEC – A generalized distinct element program for modelling jointed rock.” Final technical report to European Research Office, U. S. Army, Contract Number: DAJA37-79-C-O548, 1980.
20. Bardet JP, Scott RF. “Seismic stability of fractured rock masses with the distinct element method.” Proceedings of the 26th US Symposium on Rock Mechanics, Rapid City, SD, USA. 139-149. 1985.
21. Westergaard HM. “Water pressures on dams during earthquakes.” Transactions ASCE 1933; 98: 418-433.